FEBS Letters 476 (2000) 234–239 FEBS 23873

# Patch-clamp study of liver nuclear ionic channels reconstituted into giant proteoliposomes

Gilles Guihard[a,*], Sonia Proteau[b], Marcel Daniel Payet[b], Denis Escande[a], Eric Rousseau[b]

[a] *INSERM U533, Hôtel-Dieu, 1 Place A. Ricordeau, 44000 Nantes, France*
[b] *Department of Physiology and Biophysics, Faculty of Medicine, University of Sherbrooke, Sherbrooke, Que., Canada J1H 5N4*

Received 11 April 2000; received in revised form 7 June 2000

Edited by Maurice Montal

**Abstract Nuclear ionic channels (NICs) represent ubiquitous structures of living cells, although little is known about their functional properties and encoding genes. To characterize NICs, liver nuclear membrane vesicles were reconstituted into either planar lipid bilayers or proteoliposomes. Reconstitution of nuclear envelope (NE) vesicles into planar lipid bilayer proceeded with low efficiency. NE vesicle reconstitution into proteoliposomes led to NIC observations by the patch-clamp technique. Large conductance, voltage-gated, $K^+$-permeant and $Cl^-$-permeant NICs were characterized. An 80–105-pS $K^+$-permeant NIC with conducting sub-state was also recorded. Our data establish that NICs can be characterized upon reconstitution into giant proteoliposomes and retain biophysical properties consistent with those described for native NICs.** 

*Key words:* Nucleus; Ion channel; $Ca^{2+}$ store; Intracellular membrane

## 1. Introduction

The nucleus of eukaryotic cells is delimited by a complex nuclear envelope (NE) that is formed by two individual membranes, namely the outer and the inner nuclear membranes. These membranes are separated by a perinuclear space which is related to endoplasmic reticulum lumen. Both nuclear membranes fuse at the nuclear pore complex (NPC), where nucleocytoplasmic transport of proteins and nucleic acids occurs [1].

Both nuclear membranes and the perinuclear space exhibit complex biochemical and functional properties. The outer nuclear membrane, which is structurally and functionally related to sarco-endoplasmic reticulum (SER) membrane, possesses $Ca^{2+}$-$Mg^{2+}$ ATPase [2] which is responsible for the active transport of $Ca^{2+}$ [3–6]. Calreticulin- and calsequestrin-related proteins have been observed in the perinuclear space [7–8]. The inner nuclear membrane tightly interacts with the nucleoskeleton (lamins A, B and C) by the lamin B receptor, LAP1 and 2 proteins and emerin. Mutations in the genes encoding lamin A/C and emerin lead to Emerin-Dreyfuss dystrophy [9]. The enzymatic apparatus responsible for $InsP_3$ [10] and cyclic ADP receptor (cADPR) synthesis [11] are also described in the inner nuclear membrane. Hence, a specific pattern of expression for cyclic-nucleotide phosphodiesterases has been reported for the NE [12].

Electrophysiological properties of the NE were investigated in the early 1960s [13]. Basically, a trans-NE electrical potential exists [14], suggesting that the NE restricts ion flows, despite the presence of NPC. More recently, the presence of single nuclear ionic channels (NICs) was reported in a wide range of mammalian tissues comprising heart, liver, brain and pancreas, as well as in plant cells. A $K^+$- (200 pS) and two $Cl^-$-selective channels (180 and 58 pS, respectively) are present in liver and heart nuclear outer membrane [15,16], whereas a 166-pS $K^+$-permeant channel has been observed in the outer membrane of brain nuclei [17]. A 110-pS non-selective channel was also described in the nuclei of *Beta vulgaris* [18]. Furthermore, $Ca^{2+}$-conducting (8 pS), $Zn^{2+}$-conducting (11 pS) and cationic (30 pS) channels have been described in the inner nuclear membrane [19,20]. Despite a wealth of experiments describing NICs, little is known about their biophysical, pharmacological and molecular properties. This compromises further investigations concerning their biological roles.

In the present work, we attempted to reconstitute liver NICs into planar lipid bilayers and giant proteoliposomes. The success rate of NE fusion into planar lipid bilayers was extremely low under our conditions. By contrast, reconstitution of NE proteins into giant proteoliposomes and the use of the patch-clamp technique led to single channel characterization.

## 2. Materials and methods

### 2.1. Nuclei and NE purification

Liver nuclei were purified as previously described [19,21] with slight modifications. Dogs and rats were killed with pentobarbital (30 mg/kg). Livers were explanted, rinsed with ice-cold Tyrode solution (in mM: NaCl, 145; KCl, 4; $MgCl_2$, 1; $CaCl_2$, 1; HEPES-Na, 10; pH 7.4). The tissue (100 g) was homogenized (Waring Blendor, maximum speed, 2×30 s, 4°C) in 1 l of ice-cold buffer containing (in mM): sucrose, 320; $MgCl_2$, 3; DTT, 1; HEPES-K, 20; pH 7.2, in the presence of: Pefabloc (50 μM), pepstatin (1 μM), leupeptin (1 μM) and aprotinin (2.4 U/ml). The homogenate was twice filtered through two and four layers of cheesecloth and centrifuged in a JA15 rotor (4000×*g*, 20 min, 4°C). The pellet was resuspensed in 250 ml of buffer containing (in mM): sucrose, 2400; HEPES-K, 10; $MgCl_2$, 3; DTT, 1; with the cocktail of protease inhibitors, and subsequently centrifuged (Beckman rotor 42.1 Ti, 50 000×*g*, 90 min, 4°C). Liver nuclei appeared as a large white pellet that was gently resuspended in 50 ml of (in mM): KCl, 150; $MgCl_2$, 3; HEPES-K, 10; pH 7.2. Nuclei were concentrated by centrifugation (150×*g* for 10 min, 4°C), then resuspended in 150 mM KCl, 3 mM $MgCl_2$, 10 mM HEPES-K (pH 7.2) at $\sim 10^{10}$ nuclei per ml and finally frozen in liquid $N_2$ before conservation at −80°C.

The NE was purified as follows. Nuclei (final concentration $10^9$/ml

*Corresponding author. Fax: (33)-2-40 08 75 23.
E-mail: gilles.guihard@nantes.inserm.fr

*Abbreviations:* NE, nuclear envelope; NIC, nuclear ionic channel; NPC, nuclear pore complex; SER, sarco-endoplasmic reticulum

0014-5793/00/$20.00 
PII: S0014-5793(00)01752-X

in 150 mM KCl, 10 mM HEPES-K (pH 7.2) were sonicated twice (Branson Sonicator, pulse mode, 30 s, 4°C) in the presence of DNase I (10 μg/ml) and bovine pancreatic RNase (10 μg/ml). After 30 min incubation at 37°C, the ionic strength of the medium was increased with NaCl (1.8 M, final concentration) [7]. The NE vesicles were sedimented (100 000×*g*, 45 min, 4°C), resuspended in 150 mM KCl, 10 mM HEPES-K (pH 7.2) and frozen in liquid $N_2$ before storage at −80°C (∼2 mg protein/ml as determined by protein assay using bovine serum albumin as a standard).

### 2.2. Electron microscopy

Nuclei and NE vesicles were treated as indicated in [19] with slight modifications. In brief, samples were pre-warmed to 37°C and then stirred with a solution containing 150 mM KCl, 4% agarose (w/v) and 5 mM HEPES-KOH (pH 7.2). Agarose polymerization was induced by cooling the mixture at room temperature for 30 min. The samples were fixed for 2 h in ice-cold 0.1 M sodium-cacodylate buffer containing 2.8% glutaraldehyde (pH 7.2), then postfixed with 2% (w/v) $OsO_4$ in 0.1 M Na-cacodylate (pH 7.2). Samples were then dehydrated in grade series of ethanol solutions and embedded in EPON. Ultrathin section were stained with uranyl acetate followed by lead citrate treatment. The preparations were examined at different magnifications with a Philips EM300 electron microscope operated at 80 keV.

### 2.3. Giant proteoliposome formation

The procedure for proteoliposome formation was performed as previously described [22]. NE vesicles were mixed with asolectin at various asolectin/protein ratios. The suspension was twice frozen into liquid $N_2$ and thawed at room temperature. Aliquots (10 μl) were spotted onto Petri-dishes, dehydrated under vacuum (30 min, 4°C) and rehydrated (2 h, 4°C) with 20 μl of a solution containing (in mM): KCl, 150; $MgCl_2$, 20; HEPES-K, 10 (pH 7.2). Two ml of 50 mM KCl, 10 mM HEPES-K (pH 7.2) were added to the suspension at the end of the rehydration procedure. The giant proteoliposomes formed under these conditions were incubated for at least 1 h at room temperature to promote their attachment. Unattached proteoliposomes were removed from the dish by pipetting 1 ml of the bathing medium.

### 2.4. Single channel recording and data analysis

Patch-clamp pipettes were made by putting pyrex capillaries onto a vertical puller (Sutter Instr., Novato, CA, USA). Typical pipettes used in our experiments had 5–10 MΩ resistance (filled with 150 mM KCl). Giga-ohm seals were performed on unilamellar liposomes using pipettes filled with (in mM): KCl, 150; HEPES-K, 5 (pH 7.2), in the absence of exogenous EGTA, $Ca^{2+}$ or $Mg^{2+}$. In some experiments, KCl was substituted by K-gluconate (200 mM). After patch excision and rapid air–water interfacing, unitary currents were recorded under voltage clamp conditions [23] by using an Axopatch-1D amplifier (Axon Instruments) and stored on digital audio tapes (DTR 1802, Biologic). Data were filtered through an 8-pole Bessel filter and digitized using Aquis1 4.0 software kindly provided by G. Sadoc (URA CNRS 1131, Gif sur Yvette, France). Current analysis was performed on a personal computer using Releccan (G. Sadoc, CNRS 1131, Gif sur Yvette, France). Under our conditions, the applied potential ($V_m$) corresponded to the electrical potential of the pipette ($V_p$) minus the electrical potential of the bathing medium ($V_b$) virtually grounded to 0 mV: $V_m = V_p - V_b$.

Planar lipid bilayer experiments were performed exactly as described previously for vesicles derived from the cardiac NE [19].

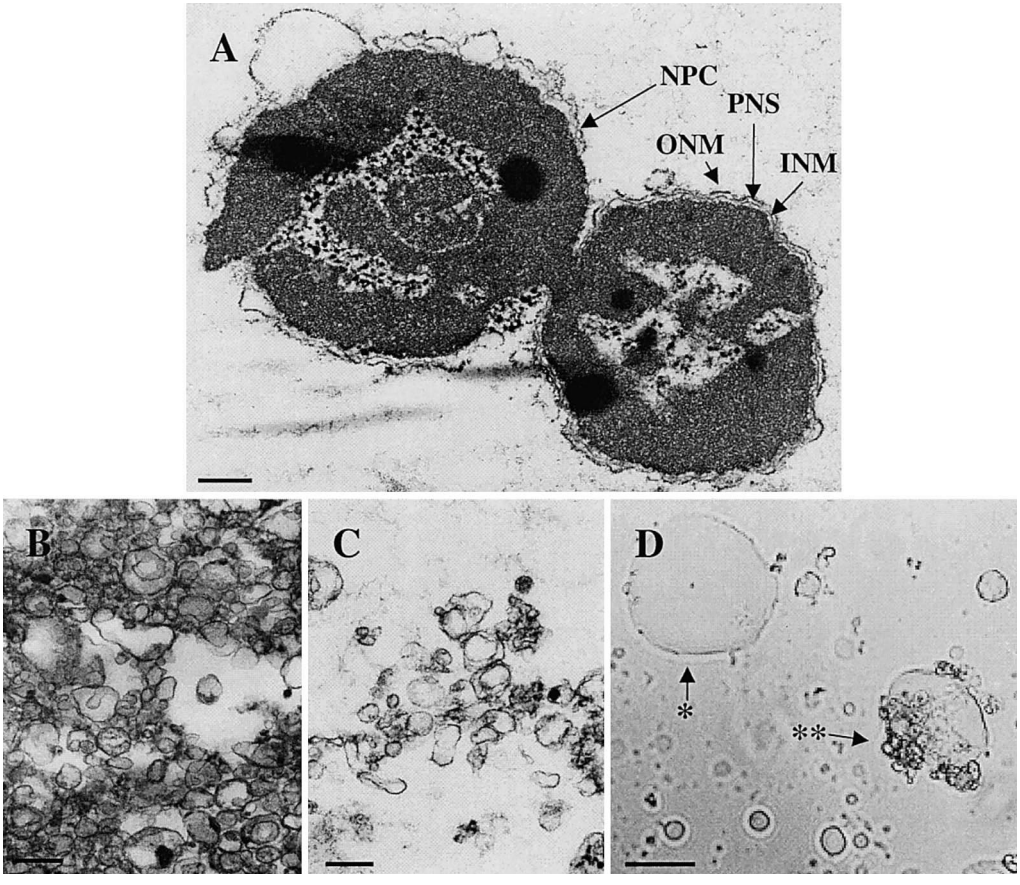


Fig. 1. Electron microscopy of liver nuclei, NE vesicles and giant proteoliposome preparations. The membrane fractions were produced as described in Section 2. A: Ultrathin section of canine liver nuclei resuspended in an agarose-containing buffer prior to fixation and electron microscopy observations. Inner nuclear membrane (INM), outer nuclear membrane (ONM), perinuclear space (PNS) and nuclear pore complex (NPC) are indicated. Calibration bar: 0.5 μm. B: Ultrathin section of a pellet of purified NE vesicles. Bar: 0.1 μm. C: NE vesicles dispersed into an agarose sodium-cacodylate buffer. Bar: 0.1 μm. D: Unilamellar (*) and complex (**) giant proteoliposomes obtained upon mixing and fusion of asolectin-liposomes and NE vesicles. Calibration bar: 30 μm.

*2.5. Chemicals*

Protease inhibitors were obtained from Boehringer (Mannheim, Germany). All other materials were of reagent grade. All buffer solutions were prepared with deionized water from a Millipore system ($18 \pm 0.2$ MΩ/cm$^2$)

## 3. Results

*3.1. Electron microscopy characterization of canine liver nuclei and NE*

Dog liver nuclei fraction exhibited a high degree of purification, since basically no contamination by other intracellular organites was detected on the basis of electron microscopy criteria (Fig. 1A) and Western blot analysis with specific nuclear-protein markers, such as lamin $B_1$ and p62 antibodies, as demonstrated in a previous report [21]. Nuclei exhibited typical NEs composed of an inner and an outer nuclear membrane surrounding nucleoplasmic condensed chromatin as shown in Fig. 1A. Note that the outer nuclear membrane retained ribosomes at its surface. Liver nuclear membrane vesicles were obtained from sonicated NEs (Fig. 1B). The vesicles had $77 \pm 14.9$ nm mean diameter ($n = 545$). Even after their dispersion into agar medium, prior to electron microscopy observation, most of the liver NE vesicles did not appear as individual entities but rather as interconnected structures (Fig. 1C). Multi-lamellar vesicles were also observed in NE preparations (Fig. 1C). Fig. 1D show the typical aspect and structure of giant proteoliposomes, formed upon mixing and fusion of asolectin liposomes with vesicles derived from the NE. As shown, proteoliposomes can be regular as well as more complex, multilamellar and branched structures.

*3.2. Detection of NICs in giant proteoliposomes*

Initial experiments were performed in order to fuse rat liver NE vesicles into planar lipid bilayer. This approach was disappointing since only two fusion events over 106 trials were observed. One of the two ionic channels recorded under these conditions corresponded to a 96-pS $Cl^-$-conducting, voltage-regulated channel (data not shown). This very low success rate was attributed to the presence of residual chromatin (DNA) and/or nucleoskeletal proteins such as lamins, surrounding the vesicles [19] and to the low density of single NE vesicles after the purification procedure.

An alternative strategy involving the formation of giant proteoliposomes was envisioned. Patch-clamp pipettes were applied to either bare liposomes (as controls) or proteoliposomes. In bare asolectin-made giant liposomes, no channel activity ($n = 6$) was ever detected over a large voltage-range; from −80 to +80 mV (Fig. 2A). When asolectin was mixed with NE vesicles, electrical activities corresponding to NIC opening and closure were consistently recorded, most of them displaying a rapid gating and the presence of sub-conducting levels (Fig. 2B). Even when an asolectin–protein ratio of 10 was used, most recordings resulted in multi-NIC traces (12 over 15 trials). Fig. 2B illustrates a typical recording obtained under symmetrical KCl (150/150 mM) conditions. Electrical activities corresponded to 225-, 108- and 53-pS conducting NICs, respectively (Fig. 2C).

*3.3. Properties of reconstituted $K^+$- and $Cl^-$-permeant NICs*

Giant proteoliposomes were obtained with an asolectin/NE–protein ratio of 50 or 100. The occurrence-frequency of

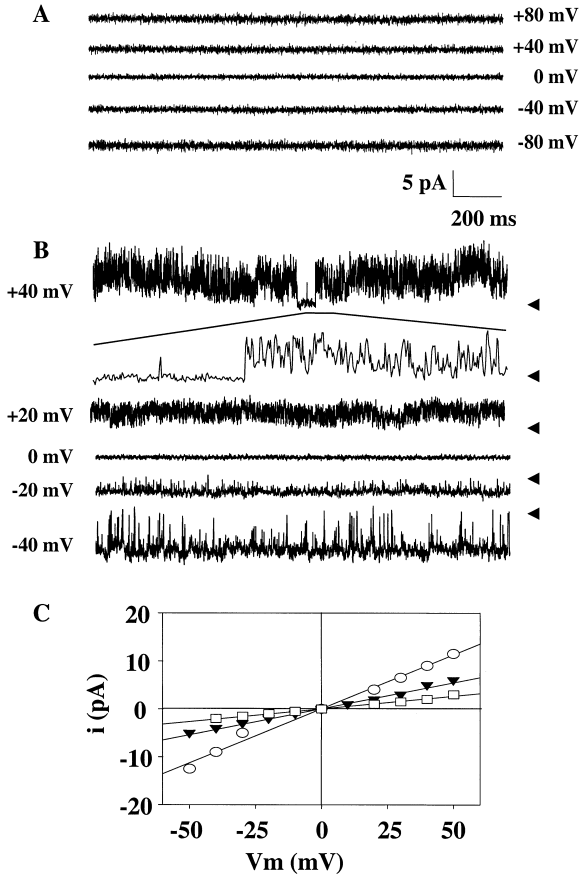


Fig. 2. Electrophysiological recordings from giant liposomes and proteoliposomes. A: Control patch-clamp recordings of asolectin-made giant liposomes, obtained in symmetrical 150 mM KCl solution. Holding potentials are indicated on the right of this panel. Under these conditions, no steady state channel activity was ever recorded. B: Recording of a unitary or multiple channel activity from a giant proteoliposome (asolectin/protein ratio = 10 w/w). Holding potentials are indicated on the left. For each trace (except at 0 mV), the zero current baseline is indicated by leftward arrowheads. C: Current–voltage relationship deduced from current level analysis of the traces illustrated in B. Current traces illustrated in A and B were filtered at 320 Hz and digitized at 1 kHz as described in Section 2.

unitary channel activities was 32.9% (65 over 228 trials). Fig. 3 illustrates the properties of a dog liver $K^+$ NIC recorded in asymmetrical (150/50 mM KCl) and in symmetrical (150/150 mM) KCl buffer systems (Fig. 3A,B, respectively). In asymmetrical 150/50 mM KCl, the zero current potential for unitary currents was found at −22 mV (Fig. 3C). From the GHK equation, a $P_{K^+}/P_{Cl^-}$ ratio of 9.4 was calculated, indicating the $K^+$ selectivity for this channel. The channel displayed large unit conductances under both symmetrical and asymmetrical conditions, of $205 \pm 12$ pS ($n = 5$) and $185 \pm 7$ pS ($n = 5$), respectively (Fig. 3C). A conducting sub-state, corresponding to 48% of the main conductance state was consistently observed, although no obvious relation between membrane potential and sub-state occurrence, could be highlighted. In contrast, the main open state of canine liver $K^+$ NIC exhibited a voltage-dependence, with negative membrane potentials increasing channel open probability (Fig. 3D).

Using a similar approach, the properties of anionic NICs

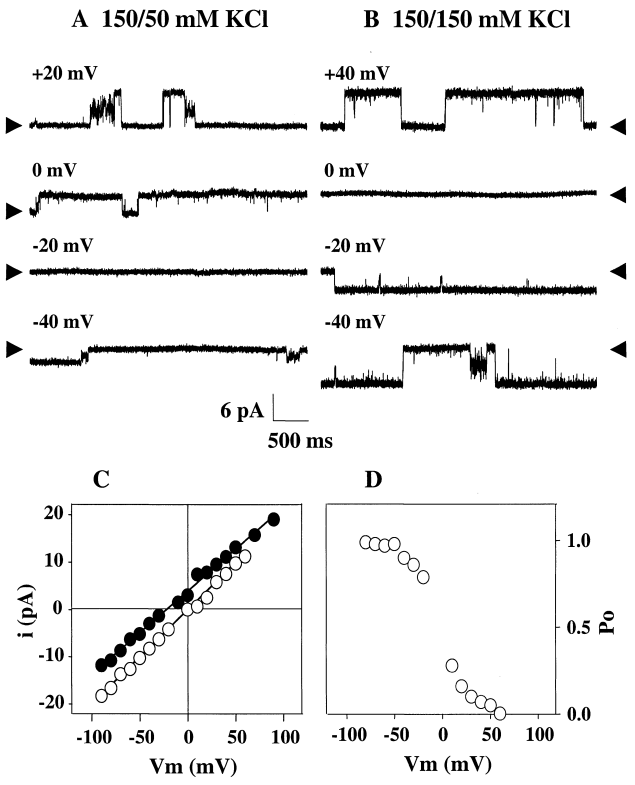


Fig. 3. Recording of a large conductance, $K^+$-selective NIC. Giant proteoliposomes were formed using an asolectin/protein ratio = 50 w/w. Unitary currents were acquired in asymmetrical (A) and in symmetrical (B) KCl buffer systems at various holding potentials. For each trace the baseline level is indicated by arrowheads. Current traces illustrated in A and B were filtered at 640 Hz and digitized at 2.5 kHz. C: Current–voltage relationships derived from the above corresponding recordings, in asymmetrical 150/50 mM (●) and symmetrical 150/150 mM (○) KCl, respectively. D: Open probability as a function of potential determined in symmetrical condition. Note that $P_0$ values were determined from 1 min duration files.

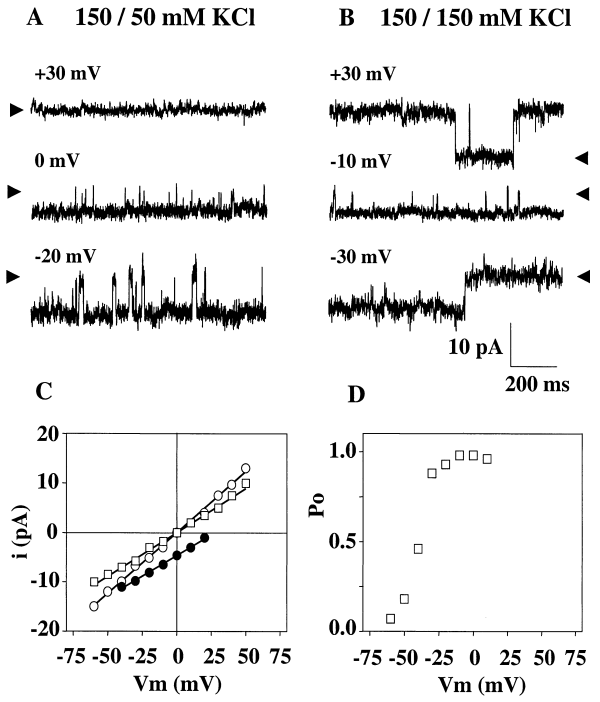


Fig. 4. Patch-clamp recording of a large conductance, $Cl^-$-selective, voltage-gated NIC. Giant proteoliposomes were formed using an asolectin/protein ratio = 50. Current traces were obtained either in asymmetrical (A) or symmetrical (B) KCl buffer and at various holding potentials as indicated on each panel. The baseline level is indicated by an arrowhead. Current traces illustrated in A and B were filtered at 1 kHz and digitized at 3 kHz. C: Current–voltage relationships derived from current amplitude analysis in asymmetrical 150/50 mM KCl (●) and in symmetrical 50/50 mM (□) or 150/150 mM (○) KCl conditions. D: Open probability as a function of voltage determined in symmetrical 50/50 mM KCl conditions. $P_0$ values were measured on 1 min duration files.

were also investigated as illustrated in Fig. 4. Unitary currents corresponding to $Cl^-$-permeant NICs were recorded in asymmetrical (150/50 mM; Fig. 4A) and symmetrical (150/150 mM; Fig. 4B, or 50/50 mM, traces not shown) KCl buffer systems. The channel displayed a mean conductance value of 171 ± 4 pS ($n = 7$), with no detectable sub-state (Fig. 4C). Channel open probability was dependent on the membrane potential with positive potentials facilitating channel opening (Fig. 4D). Superfusion of the channel under asymmetrical (150/50 mM) KCl conditions yielded a positive zero current potential of +27.3 mV (Fig. 4C) with a $P_{Cl^-}/P_{K^+}$ ratio of 80, indicative of a high $Cl^-$ selectivity over $K^+$.

The activity of a NIC, with an intermediate mean conductance of 92 ± 5 pS ($n = 4$), was also detected in an asymmetrical (200/50 mM; Fig. 5A) and a symmetrical (200/200 mM; Fig. 5B) K-gluconate buffer system to minimize the contribution of $Cl^-$-selective channels. The activity run-down was observed in the 60 s following patch excision, thus ruling out further biophysical characterization. However, a conducting sub-state at 42% of the main open state, was observed in both ionic conditions. Moreover, a zero current potential shift of −33 mV was calculated (Fig. 5C) under asymmetrical K-gluconate conditions, which was indicative of the $K^+$ selectivity of this NIC ($P_{K^+}/P_{Glu^-} = 35.8$).

The number and percentage of observations of the different NICs are given in Table 1: large conductance NICs, selective to either $K^+$ or $Cl^-$, were more frequently observed than intermediate conductance NICs. This can reflect NIC densities in native nuclear membranes, as described previously for cardiac intracellular channels [19], or result from a better structural stability of these channels during the giant proteoliposome formation procedure.

Table 1
Number and percentage of NIC observation after NE reconstitution into giant proteoliposomes

| | Number of observations |
|---|---|
| 205 pS $K^+$-selective | 26 (40%) |
| 171 pS $Cl^-$-selective | 32 (49.2%) |
| 92 pS $K^+$-selective | 7 (10.8%) |
| Total | 65 (100%) |

464 pipettes were applied onto giant proteoliposomes formed with an asolectin/protein ratio of 50 or 100. 228 patches retained gigaohm seal resistance after membrane excision and air–water interfacing. Among them, 65 contained single channel activity. The percentage of observations for each NIC category is indicated in brackets.

## 4. Discussion

Despite the number of studies devoted to the analysis of

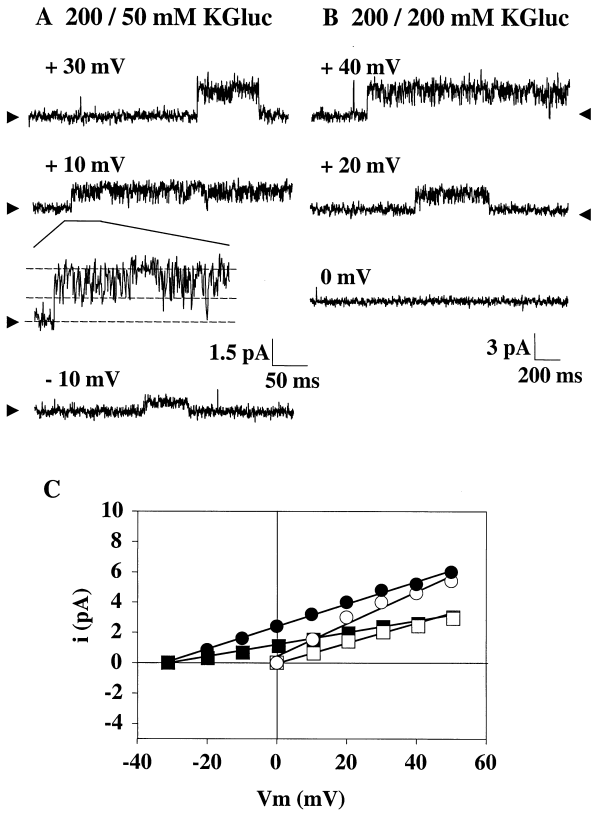


Fig. 5. Intermediate conductance, cation-selective NIC. Giant proteoliposomes were formed using an asolectin/protein ratio = 100. Current traces were obtained in asymmetrical (A) and in symmetrical (B) K-gluconate buffer systems at various holding potentials as indicated on each panel. The baseline levels are indicated by an arrowhead. Current traces illustrated in A and B were filtered at 640 Hz and digitized at 2.5 kHz. C: Current/potential curves of the intermediate $K^+$-selective NIC, determined in asymmetrical (●, ■) and in symmetrical (○, □) conditions. Circles and squares correspond to the current amplitudes of full- and sub-conducting states, respectively.

NIC properties (reviewed in [24]), little is known concerning their regulation, molecular structure and pharmacology. In the present study, electrophysiological experiments were performed to confirm the presence of cationic- and anionic-selective channels in membrane vesicles derived from the liver NE and to study their properties after functional reconstitution into model membranes.

*4.1. Characterization of the nuclear membrane*

The purification procedure followed to prepare canine liver nuclei was similar to the one described earlier for mouse and rat livers and sheep heart [16,19,21]. This procedure yields a highly enriched nuclei fraction, basically devoid of cross-contamination by other intracellular organelles. Further NE purification was performed according to [19]. Surprisingly, most of the liver NE vesicles produced herein remain interconnected by electron-dense structures as assessed by electron microscopy analysis. Such structures are likely related to the NPC, since inner and outer nuclear membranes fused at the NPC [1]. Moreover, NPCs are present at a high density (10–15 pore/$\mu m^2$) in liver nuclei, which is compatible with a high rate of nucleo-cytoplasmic transport in hepatic cells [25].

*4.2. Reconstitution of cation- and anion-selective channels*

Cardiac NICs have successfully been reconstituted into planar lipid bilayers and various NIC activities have been recorded under different conditions [19]. In our case, it was extremely difficult to fuse NE vesicles derived from canine liver nuclei. An explanation for such a discrepancy might involve the clustering of NE vesicles, the low density of single vesicles, as well as the presence of residual chromatin and/or nuclear proteins (histones or lamins) which would prevent the fusion events with the bilayer.

Giant proteoliposomes have largely been used to study channel proteins from prokaryotic [26–27] and eukaryotic intracellular membranes by the patch-clamp technique [22,28]. Such an experimental approach was also developed for plant NIC analysis [29]. Our study shows that ion channels from canine liver nuclei can be functionally characterized by means of giant proteoliposomes.

Conductance, voltage-dependence and ion selectivity of both large conductance ionic channels are in good agreement with previous observations describing native voltage-gated, large conductance $K^+$-permeant and $Cl^-$-permeant NICs in brain, cardiac and hepatic outer nuclear membrane [15–17,30]. Thus, it is likely that the activities described herein, originate from functionally reconstituted NICs in the chimeric membranes.

Do NICs belong to the NPC? Previous investigations of NEs have highlighted the NPC electrophysiological behavior complexicity, since small (i.e. 50 pS) to very large conductance (i.e. 1000 pS) activities were recorded from nucleus-attached patch [25,29,31,32]. We never detected any nS conductances upon reconstitution of canine liver NE vesicles into giant proteoliposomes. Although our experimental conditions cannot rule out the reconstitution of NPC components during proteoliposome formation, we favor the hypothesis that NICs described herein correspond to molecular entities unrelated to NPC. This is supported by data obtained from cardiac NE vesicle reconstitution in planar lipid bilayers [19] and further supported by the molecular identification of NCC27, a $Cl^-$-permeant NIC unrelated to nucleoporins [33].

Are NICs related to other intracellular ionic channels? It is known for a long time that large conductance channels with distinct cationic and anionic selectivities, are present in the SER membranes of excitable and non-excitable cells. Furthermore, it is well established that outer nuclear membrane is structurally and functionally related to the SER membrane system [2,7,34,35] although the continuum between the perinuclear space and reticulum lumen can be interrupted by an increase of cytosolic $Ca^{2+}$ [36]. The properties (i.e. conductance, conducting sub-state, ion selectivity and gating) of the 185–205-pS $K^+$ NIC recorded in our conditions, are in good agreement with those of the 200-pS conducting $K^+$ channels from skeletal muscle, diaphragm and cardiac sarcoplasmic reticulum [28,37]. The characterization of a large conductance $Cl^-$-conducting channel from rat hepatocyte endoplasmic reticulum and rabbit skeletal muscle sarcoplasmic reticulum was reported [38,39]. Electrophysiological properties of such a channel are very close to those of the large conductance $Cl^-$-selective NICs described above (Fig. 4). It is thus likely that nuclear large conductance $K^+$- and $Cl^-$ channels are related to ionic channels from SER membrane. The presence of an intermediate conductance (92 pS) cation-selective channel in the liver NE is questionable. On the one hand, it may be

related to the 125-pS, $K^+$-selective, TEA-, $InsP_3$- and $InsP_4$-insensitive channel described by Stehno-Bittel et al. [24] in *Xenopus* oocyte. However, these authors did not report any conducting sub-state for such a channel. On the other hand, this cationic channel might be related to channel protein derived from the inner membrane of the cardiac NE reported previously [19] or to a yet unidentified NIC or a specific nucleoporin.

Are NIC activities related to physiological functions? The prevailing hypothesis for the presence of large conductance monovalent cationic and anionic channels in SER membranes relates to the mechanism providing efficient counter-charge transport systems, during either $Ca^{2+}$ fluxes or protein transport. Such an hypothesis was accredited by recent results from Kargacin's group, showing that $Cl^-$ channel blockers inhibit $Ca^{2+}$ uptake by SER [40]. ATP-dependent $Ca^{2+}$ uptake and $InsP_3$- as well as cADPR-dependent $Ca^{2+}$ release have been described in the NE [5,41]. Therefore, one may propose that some, but not all, NICs are likely to be involved as a counter-charge transport system. Since a strong correlation between the $Ca^{2+}$ level of perinuclear space and the nucleo-cytoplasmic transport of macromolecules has been established [42,43], the proper and highly coordinate function of NICs may represent a crucial activity for cell physiology.

In conclusion, we provide evidence that the liver nuclei contains typical channel proteins, whose biophysical properties are compatible with those described previously on related intracellular membrane structures. Further studies are warranted to elucidate the exact biological implication/or role of this mixed population of channel proteins present in the membranes of mammalian cell nuclei. Also, investigations will be performed to resolve the biophysical properties of the InsP3-gated channel present in the membranes of NEs, described by us and others [5,6,21].

*Acknowledgements:* The electron microscopy analysis was performed at the Electron Microscopy core facility with the help of P. Magny (Université de Sherbrooke, Que., Canada). This work was supported by an INSERM-FRSQ exchange program, the France-Québec Santé Network and by the HSFQ. E.R. is a national scholar of the FRSQ.

## References

[1] Davis, L.I. (1995) Annu. Rev. Biochem. 64, 865–896.
[2] Lanini, L., Bachs, O. and Carafoli, E. (1992) J. Biol. Chem. 267, 11548–11552.
[3] Nicotera, P., Orrenius, S., Nilsson, T. and Berggren, P.O. (1990) Proc. Natl. Acad. Sci. USA 87, 6858–6862.
[4] Malviya, A.N., Rogue, P. and Vincendon, G. (1990) Proc. Natl. Acad. Sci. USA 87, 9270–9274.
[5] Gerasimenko, O.V., Gerasimenko, J.V., Tepikin, A.V. and Petersen, O.H. (1995) Cell 80, 439–444.
[6] Hennager, D.J., Welsh, M.J. and DeLisle, S. (1995) J. Biol. Chem. 270, 4959–4962.
[7] Gilchrist, J.S. and Pierce, G.N. (1993) J. Biol. Chem. 268, 4291–4299.
[8] Czubryt, M.P., Ramjiawan, B., Gilchrist, J.S., Massaeli, H. and Pierce, G.N. (1996) J. Mol. Cell Cardiol. 28, 455–465.
[9] Morris, G.E. and Manilal, S. (1999) Hum. Mol. Genet. 8, 1847–1851.
[10] Divecha, N. and Irvine, R.F. (1995) Cell 80, 269–278.
[11] Adebanjo, O.A., Anandatheerthavarada, H.K., Koval, A.P., Moonga, B.S., Biswas, G., Sun, L., Sodam, B.R., Bevis, P.J., Huang, C.L., Epstein, S., Lai, F.A., Avadhani, N.G. and Zaidi, M. (1999) Nat. Cell Biol. 1, 409–414.
[12] Lugnier, C., Keravis, T., Le Bec, A., Pauvert, O., Proteau, S. and Rousseau, E. (1999) Biochim. Biophys. Acta 1472, 431–446.
[13] Bustamante, J.O. (1994) J. Membr. Biol. 138, 105–112.
[14] Loewenstein, W.R., Kanno, Y. and Ito, S. (1966) Ann. N. Y. Acad. Sci. 137, 708–716.
[15] Mazzanti, M., DeFelice, L.J., Cohn, J. and Malter, H. (1990) Nature 343, 764–767.
[16] Tabares, L., Mazzanti, M. and Clapham, D.E. (1991) J. Membr. Biol. 123, 49–54.
[17] Draguhn, A., Borner, G., Beckmann, R., Buchner, K., Heinemann, U. and Hucho, F. (1997) J. Membr. Biol. 158, 159–166.
[18] Grygorczyk, C. and Grygorczyk, R. (1998) Biochim. Biophys. Acta 1375, 117–130.
[19] Rousseau, E., Michaud, C., Lefebvre, D., Proteau, S. and Decrouy, A. (1996) Biophys. J. 70, 703–714.
[20] Longin, A.S., Mezin, P., Favier, A. and Verdetti, J. (1997) Biochem. Biophys. Res. Commun. 235, 236–241.
[21] Guihard, G., Proteau, S. and Rousseau, E. (1997) FEBS Lett. 414, 89–94.
[22] Criado, M. and Keller, B.U. (1987) FEBS Lett. 224, 172–176.
[23] Hamill, O.P., Marty, A., Neher, E., Sakmann, B. and Sigworth, F.J. (1981) Pfluegers Arch. 391, 85–100.
[24] Stehno-Bittel, L., Perez-Terzic, C., Luckhoff, A. and Clapham, D.E. (1996) J. Gen. Physiol. 51, 195–207.
[25] Tonini, R., Grohovaz, F., Laporta, C.A. and Mazzanti, M. (1999) FASEB J. 13, 1395–1403.
[26] Delcour, A.H., Martinac, B., Adler, J. and Kung, C. (1989) Biophys. J. 56, 631–636.
[27] Berrier, C., Coulombe, A., Houssin, C. and Ghazi, A. (1989) FEBS Lett. 259, 27–32.
[28] Hirashima, N. and Kirino, Y. (1988) Biochim. Biophys. Acta 946, 209–214.
[29] Matzke, A.J., Behensky, C., Weiger, T.V.V. and Matzke, M.A. (1992) FEBS Lett. 302, 81–85.
[30] Innocenti, B. and Mazzanti, M. (1993) J. Membr. Biol. 131, 137–142.
[31] Bustamante, J.O. (1993) Biophys. J. 64, 1735–1749.
[32] Mazzanti, M. (1998) News Physiol. Sci. 13, 44–50.
[33] Valenzuela, S.M., Martin, D.K., Por, S.B., Robbins, J..M., Warton, K., Bootcov, M.R., Schofield, P.R., Campbell, T.J. and Breit, S.N. (1997) J. Biol. Chem. 272, 12575–12582.
[34] Matsuura, S., Masuda, R., Omori, K., Negishi, M.C. and Tashiro, Y. (1981) J. Cell Biol. 91, 212–220.
[35] Savory, J.G., May, D., Reich, T., La Casse, E.C., Lakins, J., Tenniswood, M., Raymond, Y., Hache, R.J., Sikorska, M. and Lefebvre, Y.A. (1995) Mol. Cell Endocrinol. 110, 137–147.
[36] Subramanian, K. and Meyer, T. (1997) Cell 89, 963–971.
[37] Picher, M., Decrouy, A. and Rousseau, E. (1996) Biochim. Biophys. Acta 1279, 93–103.
[38] Kourie, J.I., Laver, D.R., Junankar, P.R., Gage, P.W. and Dulhunty, A.F. (1996) Biophys. J. 70, 202–221.
[39] Eliassi, A., Garneau, L., Roy, G. and Sauve, R. (1997) J. Membr. Biol. 159, 219–229.
[40] Pollock, N.S., Kargacin, M.E. and Kargacin, G.J. (1998) Biophys. J. 75, 1759–1766.
[41] Santella, L. and Kyozuka, K. (1997) Cell Calcium 22, 11–20.
[42] Greber, U.F. and Gerace, L. (1995) J. Cell Biol. 128, 5–14.
[43] Perez-Terzic, C., Pyle, J., Jaconi, M., Stehno-Bittel, L. and Clapham, D.E. (1996) Science 273, 1875–1877.